Volume 2 | Number 39 | 21 October 2014 | Pages 6677–6894

Journal of Materials Chemistry B

Materials for biology and medicine

www.rsc.org/MaterialsB

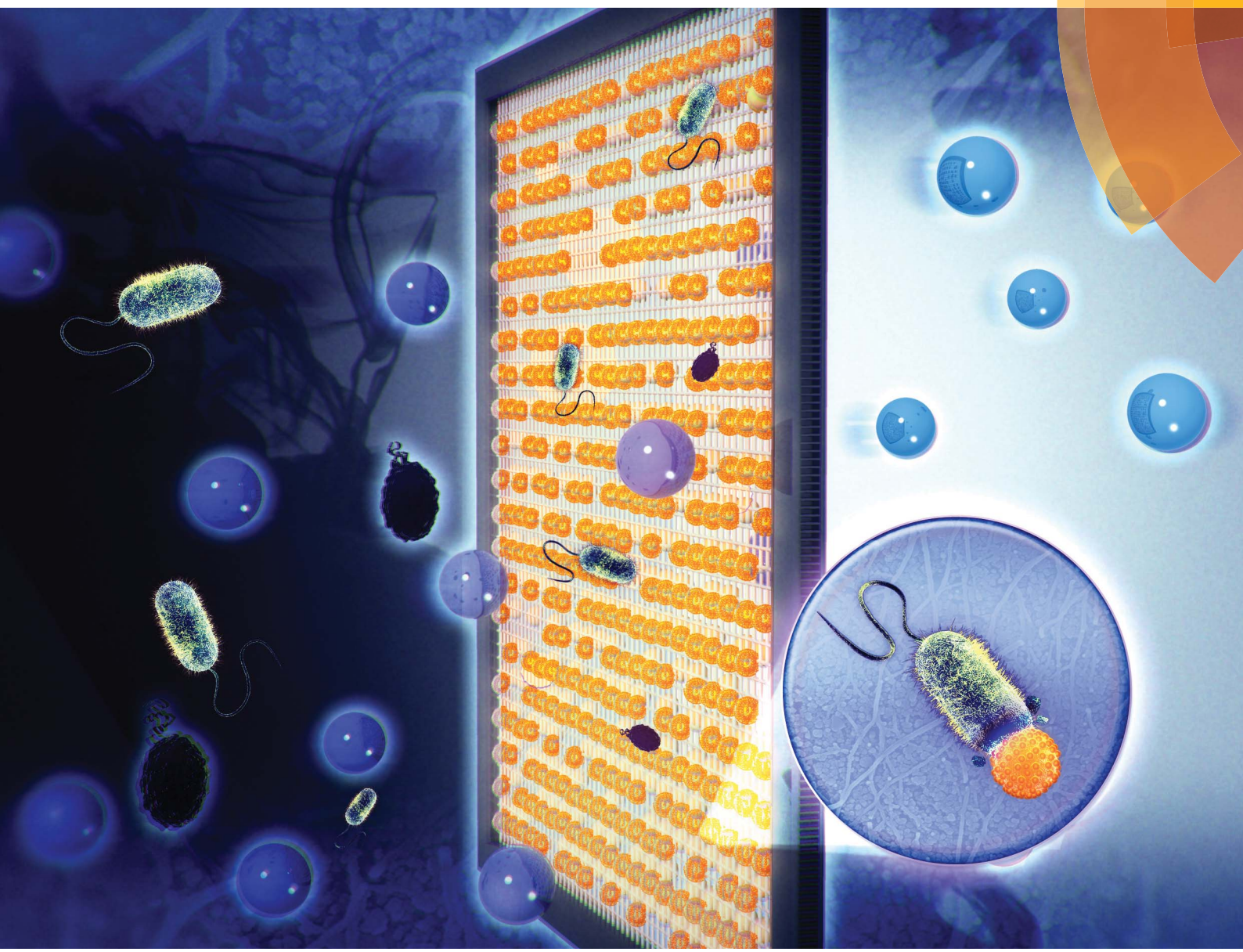

ISSN 2050-750X

ROYAL SOCIETY OF CHEMISTRY

PAPER

Kyoungja Woo *et al.*

Prompt and synergistic antibacterial activity of silver nanoparticle-decorated silica hybrid particles on air filtration

Journal of Materials Chemistry B

PAPER

View Article Online
View Journal | View Issue

Cite this: J. Mater. Chem. B, 2014, 2, 6714

Prompt and synergistic antibacterial activity of silver nanoparticle-decorated silica hybrid particles on air filtration†

Young-Seon Ko,[a] Yun Haeng Joe,[b] Mihwa Seo,[a] Kipil Lim,[a] Jungho Hwang[b] and Kyoungja Woo*[ac]

Received 1st July 2014
Accepted 8th August 2014

DOI: 10.1039/c4tb01068j

www.rsc.org/MaterialsB

There is a significant need for materials that promptly exhibit antimicrobial activity upon contact. The large-scale fabrication of monodisperse silver nanoparticle (AgNP)-decorated silica (AgNP@SiO_2) hybrid particles, and their prompt and synergistic antibacterial activity against both the Gram-negative bacteria *Escherichia coli* and the Gram-positive bacteria *Staphylococcus epidermidis* on air filtration units are presented. Monodisperse aminopropyl-functionalized silica colloids (406 nm) were used as a support material and were hybridized with AgNPs using a seeding, sorting-out, and growing strategy with Ag seeds (1–2 nm) into ~30 nm AgNPs, successfully yielding 51 g of AgNP@SiO_2 hybrid particles. Medium filter samples (glass fiber material, 4 × 4 cm^2) were coated with AgNP@SiO_2 particles and tested for antibacterial efficacy. SEM characterization of the bacterial morphology suggested prompt and synergistic antibacterial activity against both classes of bacteria. Moreover, antibacterial efficacies >99.99% for both bacteria were obtained using a filter sample with a coating areal density of 1 × 10^8 particles per cm^2. Solutions of AgNP@SiO_2 at 1.3% were stable even after 8 months. The hybrid particle AgNP@SiO_2 and the air filter system coated with the particles are expected to be useful for future green environment applications.

Introduction

Outbreaks of infectious diseases caused by airborne microorganisms present a significant threat worldwide. As a result, antimicrobial materials have attracted great attention. The development of a material that can promptly exhibit antimicrobial activity after being coated on appliances (*i.e.* air filters, air conditioners, and paint) is highly desired because the deposited microorganisms can survive and multiply when appropriate moisture and deposited nutrient dusts are present.[1–5] The multiplied microorganisms and volatile organic compounds produced by the microbial metabolism can eventually be released into the air.[2,3,6,7] This possibility highlights the need for a material, which can promptly exhibit antimicrobial activity upon contact at its coated state on the medium. In addition to prompt antimicrobial activity, the coating material should also be amenable to large-scale fabrication with monodisperse size distribution for practical utilizations.

Silver and silver containing materials such as silver nanoparticles (AgNPs) and Ag^+ ions are known to be potent antimicrobial agents.[4–6,8–13] In particular, Ag^+ ions in aqueous solution have shown great antimicrobial activity, and their antimicrobial mechanism has been studied widely.[5,8] Ag^+ ions interact with the proteins on the bacterial membrane and penetrate into the cell, where they interact with DNA and RNA. These interactions change the structure and function of target molecules and eventually lead to cell death. Antimicrobial efficacy normally appears after treatment for 2 h to several days, depending on the Ag^+ concentration. On the other hand, the antimicrobial activity of AgNPs has been debated. A clear-cut distinction between the antimicrobial activity of AgNP and that of Ag^+ has been difficult because AgNPs are oxidized by oxygen and release Ag^+ ions. Therefore, AgNPs and Ag^+ ions always coexist in aerobic aqueous solutions.[14–16] This issue was recently investigated using poly(ethylene glycol)–thiol-coated AgNPs in an anaerobic aqueous solution to prohibit the release of Ag^+ ions.[16] It was reported that the antibacterial activity of AgNPs in the anaerobic aqueous solution mainly comes from the previously oxidized and dissolved Ag^+ ions and that the particle-specific antibacterial activity is negligible.[16] Prior to this, Sondi *et al.* reported that AgNPs make pits on the membranes of Gram-negative bacteria (*Escherichia coli*) and lead to cell death in aerobic aqueous solutions.[9] Supporting reports have indicated an enhanced antibacterial effect under the co-existence of AgNPs and dissolved Ag^+ ions, rather than Ag^+ ions alone at constant

[a]Molecular Recognition Research Center, Korea Institute of Science and Technology, P. O. Box 131, Cheongryang, Seoul 130-650, Korea. E-mail: kjwoo@kist.re.kr
[b]School of Mechanical Engineering, Yonsei University, Seoul 120-749, Korea
[c]Korea University of Science and Technology, Seoul 136-701, Korea

† Electronic supplementary information (ESI) available: A photograph of tailor-made 50 L reactor, experimental setup for fabrication of antibacterial air filters, TEM and SEM images, UV-Vis absorption spectrum. See DOI: 10.1039/c4tb01068j

concentrations.[17–19] In particular, comparable antibacterial activities of AgNPs and the released Ag^+ ions have been observed for AgNPs larger than ~15 nm,[18,19] whereas the antibacterial activity is dominated by the released Ag^+ ions for AgNPs smaller than ~10 nm.[18] It is noteworthy that AgNPs[9,17–19] which have shown enhanced antibacterial activity, in addition to the antibacterial activity of Ag^+ ions, have had a partially naked surface due to their labile ligands or their hybrid structure. Unfortunately, fully naked AgNPs cannot exist as a colloidal solution due to their aggregation caused by high surface energy.

A silica hybrid colloid encapsulating a magnetite core and decorated with 30 nm-sized AgNPs ($AgNP@SiO_2/Fe_3O_4$)[20] and a magnetite-silica Janus nanorod decorated with 5 nm-sized AgNPs ($AgNP@Fe_3O_4–SiO_2$)[21] have been reported as magnetically collectable antimicrobial materials in water. Both reports used the silica material as a biocompatible, water-dispersible, and physico-chemically stable inorganic support for the naked AgNPs. The former colloid exhibited immediate and synergistic antibacterial activity compared to the latter Janus nanorod due to the large (30 nm *vs.* 5 nm) and many AgNPs in a three-dimensional structure on a silica support.[20] However, hybridization of silica with magnetic material encumbers a synthesis process with extra complexity, particularly for a large-scale fabrication. Moreover, the magnetic property is not necessary for a coating material, which is applied on appliances such as air filters and air conditioners. Thus, monodisperse silica hybrid particles decorated with AgNPs of ~30 nm may be a reliable candidate as a prompt antibacterial coating material.

Researchers have coated Ag^+ ion-containing materials and AgNPs or their carbon composites on glasses and air filters using various methods and have reported antibacterial efficacy by the colony count method (CCM) or by the disk diffusion method (DDM), which are generally used worldwide.[4,5,13,22–26] The CCM is a method to count the bacterial colony number after spreading a specimen-treated bacterial solution on an agar plate and incubating for approximately 24 h. The DDM is based on the appearance of a belt-like inhibition zone surrounding the specimen after placing it on the nutrient agar in bacterial solution and incubating for approximately 24 h. Both methods evaluate antibacterial activity after incubation of aqueous bacterial solution with the Ag^+- or AgNP-coated specimen. Fundamentally, these evaluation methods do not differentiate the antibacterial effect of Ag^+ ions from that of AgNPs which release Ag^+ ions into aerobic water. To the best of our knowledge, there has been no substantiated coating material showing a prompt antibacterial activity in air. Therefore, a material that can promptly show antibacterial activity in air at its coated state is greatly needed.

In this report, the large-scale (51 g) fabrication of monodisperse silica hybrid particles decorated with ~30 nm-sized AgNPs ($AgNP@SiO_2$), and their prompt and synergistic antibacterial activity against both the Gram-negative bacteria *Escherichia coli* (*E. coli*) and the Gram-positive bacteria *Staphylococcus epidermidis* (*S. epidermidis*) on air filtration units are presented.

Experimental

Materials

Ethanol (Burdick & Jackson, 99.9+%), NH_4OH (Junsei, 28.0–30.0%), tetraethylorthosilicate (TEOS, Sigma Aldrich, 98%), 3-(aminopropyl)trimethoxysilane (APTMS, Sigma Aldrich, 97%), tetrakis(hydroxymethyl)phosphonium chloride (THPC, Sigma Aldrich, 80% solution in water), formaldehyde (Sigma Aldrich, 37% solution in 10–15% methanol), $AgNO_3$ (Sigma Aldrich, >99.0%), NaOH (Showa, 93.0%), and HCl (Matsunoen Chemicals Ltd., 35%) were used as purchased.

Characterization

The TEM images were recorded using a CM30 (Philips, 200 kV). The SEM images were recorded using a FEI XL30-ESEM or NOVA200 NOVA-SEM. All of the SEM samples were coated with Pd/Pt for 20 s (HITACHI, E-1010 Ion Sputter). X-ray photoelectron spectroscopy (XPS) data were obtained with a PHI 5000 VersaProbe (Ulvac-PHI) using monochromatic Al Kα radiation (1486.6 eV). For XPS sample preparation, one drop of the sample solution was placed on a silicon wafer and naturally dried. X-ray diffraction (XRD) patterns were measured by a Rigaku Dmax 2500 with Cu Kα radiation ($\lambda = 1.5406$ Å). UV-Vis spectra were recorded using a Perkin Elmer Lambda 25 with a 1 cm-cell.

Fabrication of aminopropyl-functionalized silica sphere ($_{AP}SiO_2$)

The typical Stöber process[27] with appropriate modifications was applied to fabricate silica spheres. In a tailor-made 20 L reactor with a mechanical stirrer at ambient temperature (20–25 °C), 8 L of ethanol, 0.8 L of deionized water (DW), and 0.24 L of NH_4OH were stirred. 0.48 L of TEOS was then added and stirred for 5 h, yielding ~280 nm silica spheres. Consecutively, 0.8 L of DW, followed by 0.48 L of TEOS, was added and stirred for 5 h to grow silica spheres. This step was repeated once more, yielding ~400 nm silica spheres. For aminopropyl (AP)-functionalization, 9 mL of APTMS diluted in 30 mL of ethanol was added and stirred overnight. The resultant $_{AP}SiO_2$ was centrifuged, washed with 2 L of ethanol 6 times using centrifugation, and finally dispersed in 2.5 L of ethanol. This process yielded a stock solution of 16.94% by weight/volume (16.94 g in 100 mL) with a diameter of 406 ± 17 nm (average ± standard deviation), as measured by TEM analysis.

Fabrication of $AgNP@SiO_2$

Two hundred mL of 16.94% $_{AP}SiO_2$ stock solution was centrifuged and dispersed in 100 mL of DW. By adding 400 mL of 0.1 M HCl, the solution was adjusted to pH ~ 4 and stirred for 15 h to achieve a homogeneous dispersion. To prepare Ag seeds with 1–2 nm size at ambient temperature, 720 mL of DW and 80 mL of 0.1 M NaOH solution were mixed in a 1 L Pyrex glass bottle with a cap. To this solution, 0.34 mL (1.9 mmol) of THPC was added as a reducing agent. After stirring for 2 min, 32 mL (1.9 mmol) of 1% $AgNO_3$ solution was poured in and the

solution was stirred for 15 min. Five sets of the Ag seed solution were prepared simultaneously and combined in a 5 L Pyrex glass bottle with a cap. The $_{AP}SiO_2$ solution prepared above was then poured into the 5 L bottle containing the Ag seeds and gently swirled every 30 min for Ag seeding onto the $_{AP}SiO_2$. After 2 h, the solution was centrifuged and the $Ag_{seed}@SiO_2$ solid was dispersed in 500 mL of DW. Moreover, in a tailor-made 50 L reactor (Fig. S1†) equipped with a chiller jacket for temperature control (12 ± 1 °C) and mechanical stirrer, 35 L of distilled water and 21 g of $AgNO_3$ were combined and stirred. When 21 mL of NH_4OH was added and stirred, the suspension became transparent. This indicates the formation of a $[Ag(NH_3)_2]^+$ complex, which is amenable to a controlled reduction to Ag due to its lower standard reduction potential (+0.38 V) than that of Ag^+ (+0.80 V).[19] Then, the $Ag_{seed}@SiO_2$ solution was poured into the reactor and stirred for 30 min to sort out the relatively larger seeds. The larger seeds sorted out are coalesced together and later removed by centrifugation. Next, for a controlled reduction of $[Ag(NH_3)_2]^+$ complexes to Ag and growth of remaining Ag seeds to AgNPs on $_{AP}SiO_2$, 10 mL of formaldehyde dissolved in 1 L of DW was added to the reactor slowly over 3 h through 3 openings using 3 dropping funnels while stirring. Moreover, 20 mL of formaldehyde dissolved in 200 mL of DW was added for 2 h. After further stirring for 1.5 h, the stirrer and chiller were set to the off position and the solution was left overnight without agitation. The solution was centrifuged, and the solid was washed with a 0.01% formaldehyde solution using centrifugation. Finally, the solid (51 g), which is the upper limit of yield with the reactor, was dispersed in DW to make 1 L of $AgNP@SiO_2$ solution.

Preparation of air filter samples coated with $AgNP@SiO_2$

The experimental setup for air filter coating is shown in Fig. S2.† Briefly, clean air flowing at 2 L min^{-1} entered the Collison-type atomizer, which contained a 1.3% $AgNP@SiO_2$ solution. The nanoparticles were aerosolized, and passed through a diffusion dryer for water removal. Finally, the generated particles were transported to coat the medium filters (Fabriano®, 4×4 cm^2). The size distributions of the nanoparticles upstream and downstream from the filter samples were measured using a scanning mobility particle sizer (SMPS, 3936N22 Custom, TSI Inc., St. Paul, MN, USA). The SMPS system consisted of a classifier controller (3080, TSI Inc., USA), a differential mobility analyzer (DMA, 3081, TSI Inc., USA), a condensation particle counter (CPC, 3022A, TSI Inc., USA), and an aerosol charge neutralizer (Soft X-ray charger 4530, HCT Co., Ltd., Korea) and was operated at a sampling air flow rate of 300 cm^3 min^{-1}.

The average size of the aerosols was determined to be ~430 nm by SMPS. The particle concentrations upstream and downstream from the filter samples were 1.78×10^5 particles (#) per cm^3 and 1.75×10^4 # per cm^3, respectively. The coating areal density (ρ_{areal}) in # per cm^2 was calculated using eqn (1) for each coating time t:

$$\rho_{areal}\left[\#/cm^2\right] = \frac{(C^{up} - C^{down})[\#/cm^3]\ Q[cm^3/min]\ t[min]}{A[cm^2]} \quad (1)$$

where Q is the carrier gas flow rate, A is the effective cross-sectional area of the filter sample, and C is the total mass concentration of the nanoparticles. The superscripts "up" and "down" refer to the upstream and downstream locations of the filter sample, respectively. Table 1 summarizes the various coating areal densities for different coating times. The coating areal density increased linearly with the coating time.

Preparation of bacterial solution

Two types of bacteria were selected for the antibacterial tests: *Escherichia coli* (ATCC 11775) as a Gram-negative bacterium, and *Staphylococcus epidermidis* (ATCC 14990) as a Gram-positive bacterium. Both bacteria were prepared by liquid culture, in which the desired bacteria were suspended in BD® Difco™ Nutrient Broth. This liquid broth consists of approximately 3 g of beef extract and 5 g of peptone per L. After inoculation, the bacteria were grown in the liquid broth overnight in a shaking incubator (DSS 6001, Dasol MI-Tech, Korea) at 37 °C. The bacterial media were then diluted with nutrient broth; therefore, the number of bacterial cells in the solutions was approximately 1×10^6 colony forming units (CFU) per mL.

Antibacterial test

The CCM was applied to count bacterial colony numbers as follows. More specifically, 1 mL of the bacterial culture solution was added to 9 mL of DW. A filter sample was cut into a 1 cm diameter circular shape and was then placed into the solution and incubated with shaking at 37 °C for 24 h. The incubated solution was serially diluted with DW to obtain a countable number of colonies, and 100 μL of each diluted solution was

Table 1 Summary of various coating areal densities for different coating times

Coating time t (min)	Particle concentration (# per cm^3)		Volume flow rate Q (cm^3 min^{-1})	Effective area A (cm^2)	Coating areal density ρ_{areal} (# per cm^2)
	C^{up}	C^{down}			
1	1.78×10^5	1.75×10^4	2000	16	2×10^7
3					6×10^7
5					1×10^8
10					2×10^8

spread onto the surface of 87 mm × 15 mm Petri dishes containing 15 mL of nutrient agar. The plates were then cultured in an incubator at 37 °C for 24 h, after which the number of CFUs per sample was determined by counting.

The results of each experimental method were averaged from a dozen replications. Antibacterial efficiency (η_{CCM}) was calculated by the following eqn (2):

$$\eta_{CCM} = \left(1 - \frac{CFU}{CFU_0}\right) \times 100\% \quad (2)$$

where the subscript '0' indicates the control case (*i.e.*, bacterial concentration when exposed to a filter sample without AgNP@SiO_2).

Interaction of bacteria with AgNP@SiO_2-coated air filters in air

Fifty mL of bacterial solution, which was obtained after a shaking incubation for 4 h, was centrifuged and the pellet was dissolved in 50 mL of DW. The centrifuging process was performed two more times with the same operating conditions. Then, the solution was diluted with DW to an optical density (OD) of 0.1 as measured using a photospectrometer (Libra S12, Biochrom Ltd., UK) at a wavelength of 600 nm. Fifty mL of the solution was aerosolized and deposited onto the coated air filter sample that was prepared with a coating areal density of 2×10^8 # per cm^2 using the experimental setup shown in Fig. S2.† These samples were subsequently analyzed by SEM.

Interaction of bacteria with AgNP@SiO_2 in aqueous solution

Ten mL of bacterial solution (OD = 0.1) was prepared according to the same process described for bacterial deposition onto the coated air filter. Five mL of the bacterial solution was mixed with 5 mL of 0.01% AgNP@SiO_2 solution and the mixture was incubated under shaking at 30 °C for 0, 10, and 30 min. Ten μL of incubated solution was dropped onto a silicon wafer for analysis by SEM.

Results and discussion

To serve as support materials for the hybrid structure, a large amount of silica spheres were prepared by modifying the Stöber process.[27] Briefly, silica spheres were grown successively until they reached ~400 nm and then functionalized with AP moieties in a one-pot synthesis. This process yielded 424 g of AP-functionalized silica spheres ($_{AP}SiO_2$) with diameters of 406 ± 17 nm (average ± standard deviation from TEM image in Fig. S3†). Their SEM image is shown in Fig. 1a(i). For the application of AgNP@SiO_2 hybrid materials, we have chosen an air filter with a coating system using an atomizer. Thus, an average diameter of ~400 nm was chosen to avoid the most penetrated particle size range (100–300 nm),[28] where the aerosol coating efficiency is the lowest, and to avoid aggregation, which frequently occurs with sizes smaller than ~100 nm. Fig. 1a(ii and iii) show SEM images of highly monodisperse AgNP@SiO_2 hybrid particles that were fabricated on the 51 g scale. A monodisperse coating material provides many advantages because the coating system becomes practically simple and economical due to fewer variable factors and the performance of the coated products becomes more reliable. The bright spots designating decorated AgNPs show a relatively homogeneous distribution with some distance between the particles on $_{AP}SiO_2$. The undecorated part of the $_{AP}SiO_2$ hybrid exposes AP moieties, which are essential for the water-dispersive property of the AgNP@SiO_2 hybrid colloids.

The overall process for the hybridization reaction is illustrated in Scheme 1. Fig. 1b(i–iv) show TEM images of a magnified part of each hybrid particle through the fabrication process. Corresponding TEM images of the whole hybrid particles are included in Fig. S4.† Fig. 1b(i) shows the smooth surface of a part of $_{AP}SiO_2$ and corresponds to Scheme 1a. Fig. 1b(ii) shows densely self-assembled Ag seeds on $_{AP}SiO_2$ (Ag_{seed}@SiO_2) and corresponds to Scheme 1b. The reaction for the self-assembly of Ag seeds on $_{AP}SiO_2$ was delicate and different from that of Ag seeds on $_{AP}SiO_2/Fe_3O_4$ (ref. 20) or from that of Au seeds on $_{AP}SiO_2$.[29] The labile property of a bond between an amine and an Ag seed is not considered to allow seeding by coordinative bonding, which works nicely in the case of Au seeds.[29–31] Thus, an electrostatic interaction was used to self-assemble negatively charged THPC-protected Ag seeds on a positively charged $_{AP}SiO_2$ at pH ~ 4. In the case of Ag seeding on $_{AP}SiO_2/Fe_3O_4$, the Fe_3O_4 core seems to play a role as a stabilizer for the seeded hybrid structure of Ag_{seed}@SiO_2/Fe_3O_4 thanks to its reducing property[32] with respect to Ag^+ to Ag. However, large-scale fabrication with a monodisperse size distribution is limited in the case of AgNP@SiO_2/Fe_3O_4 hybrid particles, because the silica-encapsulation reaction of the Fe_3O_4 core requires a highly diluted condition to avoid aggregation and the resultant product SiO_2/Fe_3O_4 exhibits a range (0.5–0.7 μm) of size distribution.[20] For a successful seeding on $_{AP}SiO_2$, a large portion of well-controlled Ag seeds in the 1–2 nm range was required. These seeds were obtained by optimizing the molar ratio of THPC–Ag to 1 : 1 and by adding Ag^+ into a THPC solution rather than the *vice versa*. The $_{AP}SiO_2$ solution (pH ~ 4) was poured into the alkaline THPC-protected Ag seed solution and gently swirled intermittently for seeding. When the centrifuged and re-dispersed Ag_{seed}@SiO_2 solution was poured into an Ag^+ solution containing NH_4OH and stirred, only the relatively larger seeds were displaced from the amine moieties and coalesced together as shown in Fig. 1b(iii) and Scheme 1c. The coalesced particles departed from the silica particle due to their lager inertia during stirring and at the end of the reaction they were removed by centrifugation. The stirring time of Ag_{seed}@SiO_2 with the Ag^+ solution containing NH_4OH was critical and was adjusted empirically. This kind of sorting-out step guaranteed some distance between the relatively small remaining seeds. This distance was necessary for the seeds to grow into the nanoparticles shown in the Fig. 1b(iv) and Scheme 1d. During the early stage of the growth step, the remaining Ag seeds are likely to grow in all directions. During the later stage, the seeds grow upwards and sideways because there is not much space downward. Through the growth step, AP moieties are expected to be embedded in AgNPs, similar to the case of AgNPs grown from the Au seeds.[29] Thus, the AgNPs on the $_{AP}SiO_2$ sphere

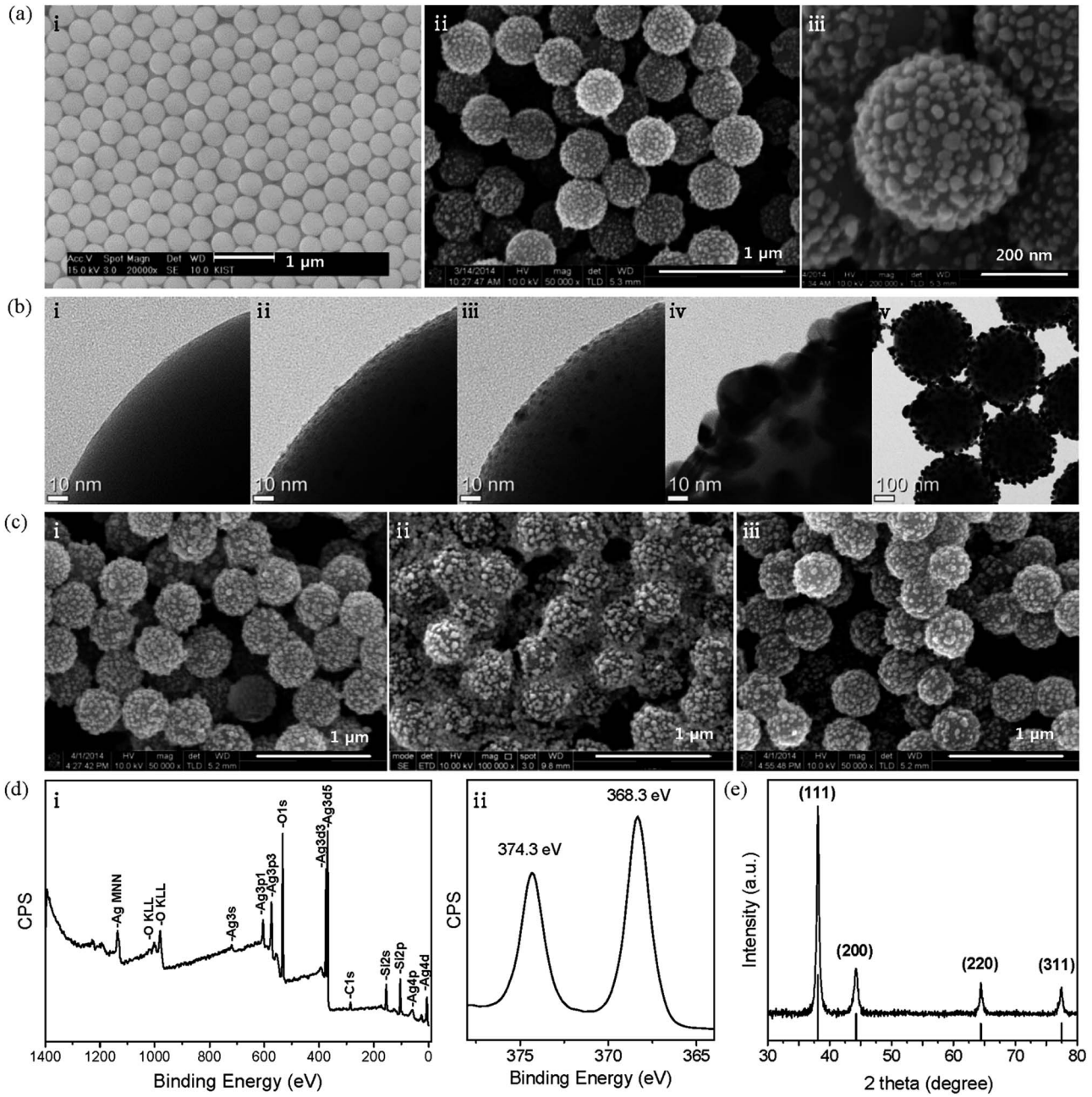

Fig. 1 (a) SEM images of (i) SiO_2 particles, (ii) AgNP@SiO_2 particles, and (iii) a single AgNP@SiO_2 particle, (b) TEM images of part of a hybrid structure for (i) initial $_{AP}SiO_2$, (ii) after Ag seeding, (iii) after sorting-out, (iv) after growing, and of (v) AgNP@SiO_2 particles, (c) SEM images of (i) 1.3% AgNP@SiO_2 solution, after 8 months, (ii) × 10 dilution, after 1 month, and (iii) × 10 dilution in 5 #% SiO_2/Fe_3O_4 solution, after 1 month, (d) XPS (i) survey scan spectrum and (ii) the corresponding specific spectrum of elemental Ag, and (e) XRD pattern of AgNP@SiO_2 particles (lines: JCPDS File no. 04-0783).

exhibit a hemisphere-like shape, which is key for the fixation of the AgNPs on $_{AP}SiO_2$ spheres. Without the sorting-out step, the densely self-assembled Ag seeds are likely to grow to a smooth and complete shell on $_{AP}SiO_2$.[29,33] In the case of using Au seeds, instead of Ag seeds, growth of the AgNPs is limited up to ~15 nm because the Au seeds pass through a different reaction pathway[29] than the Ag seeds and the resultant hybrid particles show much lower antimicrobial effects than their corresponding hybrid particles with ~30 nm AgNPs.[20] The TEM image of AgNP@SiO_2 particles exhibits gray and black areas, which correspond to silica and AgNPs, respectively.

Fig. 1c shows the stability of the hybrid structure of AgNP@SiO_2 colloids with varying times and concentrations in aqueous solution. The initial morphology of a 1.3% AgNP@SiO_2 solution was preserved after 8 months (i). In the case of a 5% solution, the initial morphology was preserved even after 1 year (data not shown). Therefore, the hybrid structure of AgNP@SiO_2 colloids in solution seems to be stable for use as an air filter

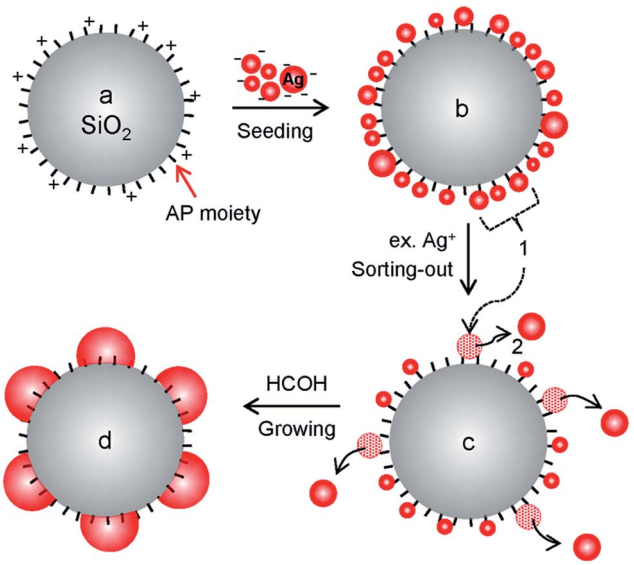

Scheme 1 Illustration for the fabrication process of an AgNP@SiO_2 hybrid particle.

coating, considering that the concentration we applied in the atomizer for air filter coating was 1.3% and a higher concentration would lead to higher throughput in the coating process. However, the 10-fold diluted hybrid colloids (0.13%) lost their integral morphology after only 1 month (ii). This morphological change was likely caused by oxidation and dissolution of AgNPs in the diluted aerobic solution. Interestingly, when SiO_2/Fe_3O_4 particles were added at 5% by particle number, the morphology was preserved (iii). The preservation of the hybrid structure of AgNP@SiO_2 colloids in (iii) can be attributed to the sacrificial oxidation of Fe^{2+} to Fe^{3+} in the Fe_3O_4 core prior to oxidation of AgNPs because the standard reduction potentials of Ag^+ to Ag and Fe^{3+} to Fe^{2+} are 0.80 V and 0.77 V, respectively.[34]

Fig. 1d shows the XPS result of an AgNP@SiO_2 sample. The carbon 1 s line was used as a reference for the binding energy scale (284.6 eV). Every line position in (i) is similar to those of AgNP@ SiO_2/Fe_3O_4,[20] as expected, because the magnetite core is located deep at the center of the hybrid sphere with a silica shell thickness of ~0.1 μm. Interestingly, however, the line positions of Ag $3d_{5/2}$ and $3d_{3/2}$ in the high resolution spectrum (ii) appear at 368.3 and 374.3 eV, which are 0.5 eV higher than those in AgNP@SiO_2/Fe_3O_4. This result indicates that partial oxidation of the AgNPs proceeded further on SiO_2 than on SiO_2/Fe_3O_4. Fortunately, it has been reported that partially oxidized AgNPs still exhibit antibacterial activity,[13,14] which will be shown later. The XRD pattern of AgNP@SiO_2 (Fig. 1e) exhibits only the face centered cubic crystalline phase of the Ag metal (JCPDS File no. 04-0783) because silica is amorphous. The UV-Vis absorption spectrum of AgNP@SiO_2 (Fig. S5†) shows a typical plasmonic peak[33] of AgNPs at 410 nm as well as the associated peak at ~600 nm.

As an example for application, AgNP@SiO_2 aerosols were generated from AgNP@SiO_2 colloidal solution *via* a Collison atomizer and coated on the air filter samples using the experimental setup in Fig. S2.† The coated filter samples with varying coating times and particle concentrations are summarized in Table 1. First, we wanted to examine whether the coated AgNP@SiO_2 particles exhibit antibacterial activity on air filtration units. For this purpose, the selected bacterial aerosols carried by clean air at 2 L min^{-1} were deposited on the AgNP@SiO_2-coated filter samples with a coating areal density of 2×10^8 # per cm^2. SEM images of these samples with different magnifications are displayed in Fig. 2a and b for *E. coli* and *S. epidermidis*, respectively. The coated AgNP@SiO_2 aerosols show a relatively homogeneous distribution on the filter. Relatively larger ellipsoids (~0.6 μm) in a and spheres (~0.8 μm) in b represent *E. coli* and *S. epidermidis*, respectively, which agrees with the published data.[35,36] Strikingly, both types of bacteria are trapped by AgNP@SiO_2 hybrid particles coated on the filter fiber and a single AgNP@SiO_2 hybrid particle is enough to trap each bacterium. Furthermore, the trapped bacteria do not seem to be viable, possibly because the trap is so strong that the bacteria cannot escape without rupturing their cellular membrane or cell wall. Many AgNPs protruding from a silica support are considered to play a key role as many teeth to bite bacteria, leading to cell death by chemsorption of Mg^{2+} or Ca^{2+} ions from bacterial surface as will be discussed later. To the best of our knowledge, this is the first explicit evidence for a coated material showing prompt antibacterial activity on air filtration.

It would be useful to know whether the interaction between AgNP@SiO_2 hybrid particles and bacteria in air is the same as in water. Thus, the temporal morphology of the bacteria was investigated while incubating their aqueous mixtures with AgNP@SiO_2 hybrid colloids. SEM images from this experiment are displayed in Fig. 2c and d and S6.† In the case of *E. coli*, their morphology (ellipsoid, a) trapped on the filter looks different from that (ci) dropped on the silicon wafer. The morphology of *E. coli* on the filter has been preserved during Pd/Pt sputtering for SEM sample preparation because they were deposited on the filter fiber in three-dimensional space after passing through a diffusion dryer. On the other hand, the dropped and dried *E. coli* on the silicon wafer with a two-dimensional surface exhibits rich surface morphology, as reported,[37] due to a chemical etching by plasma during Pd/Pt sputtering. Plasma is known to etch away the outer membrane according to the treatment time and cause shrinkage of *E. coli* (ATCC 11775).[37] The *E. coli* bacteria seem to be disrupted promptly upon contact with AgNP@SiO_2 colloids. No pristine bacteria were present, even at 10 min. In the case of *S. epidermidis*, most AgNP@SiO_2 colloids seem to bite bacteria promptly at their first contact (10 min image). In contrast to the morphology (sphere) of bacteria trapped on the coated air filter, the morphology of *S. epidermidis* on the silicon wafer exhibited an additionally flattened disk shape, which seems to be caused by the Pd/Pt sputtering on the wafer for SEM sample preparation.[37] Bitten traces are indicated as an arrow in Fig. 2d and S6b.† The bitten traces appear to be separated from the AgNPs on the silica sphere by the sputtering impact. Therefore, we deduced that the bacteria trapped on the AgNP@SiO_2 hybrid particles coated on the air filter will lead to cell disruption, indicating cell death and that many AgNPs decorated on the silica sphere play that role promptly and synergistically; *i.e.*, a single AgNP with

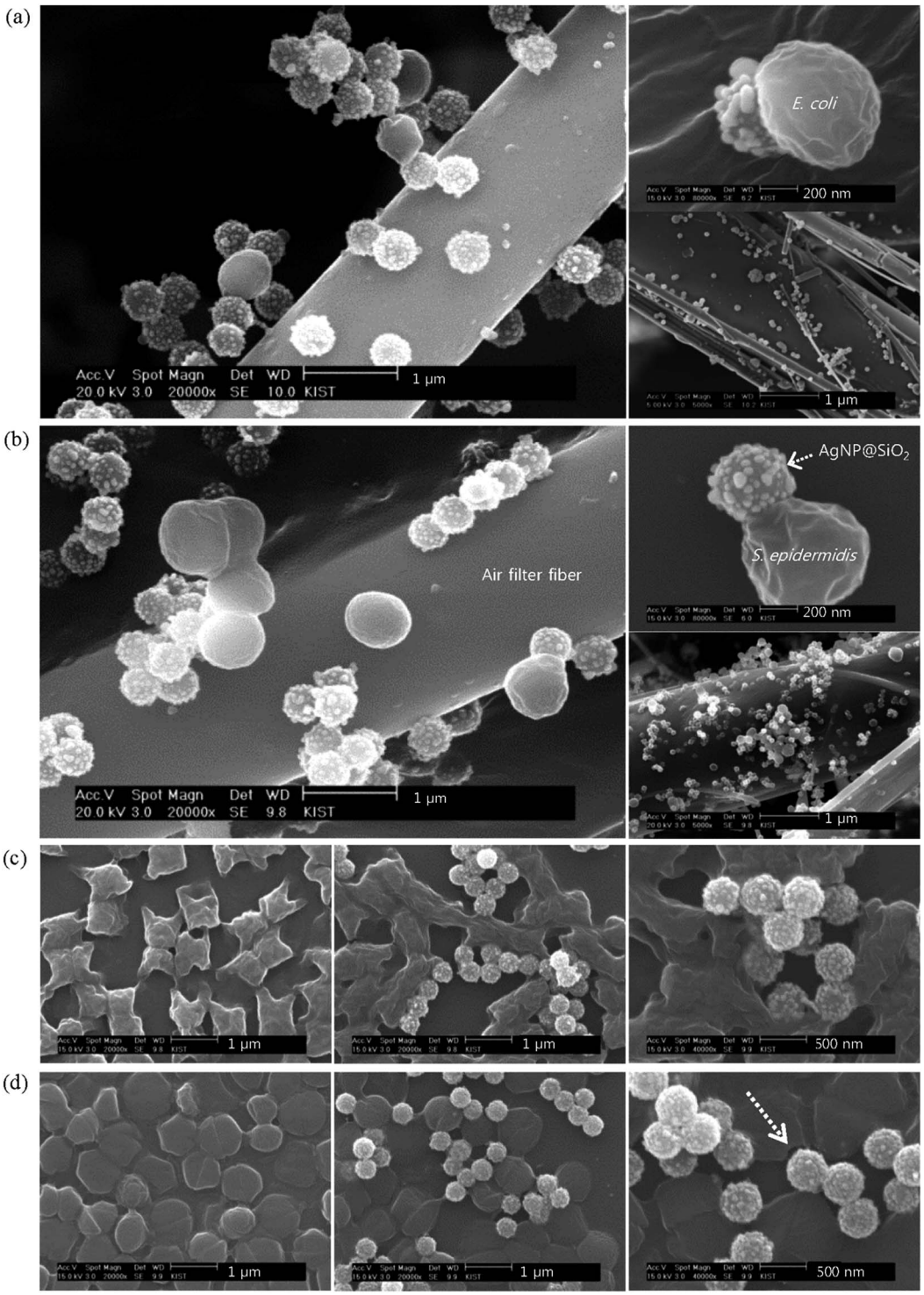

Fig. 2 SEM images of (a) *E. coli* and (b) *S. epidermidis* deposited on the AgNP@SiO_2-coated air filter at different magnifications and (c) *E. coli* and (d) *S. epidermidis* incubated in AgNP@SiO_2 solution for 0, 10, and 30 min (left, middle, and right, respectively).

partially naked surface can make a pit on the Gram-negative bacterial membrane,[9] whereas a single AgNP@SiO_2 hybrid particle can disrupt a bacterial membrane or cell wall upon contact. Cell viability tests that will be shown later with Fig. 3b and c can support our deduction. This type of prompt antibacterial effect from AgNP@SiO_2 hybrid particles may be particularly promising for treatment of antibiotic-resistant microorganisms such as super-bacteria.

The prompt and fatal antibacterial activity of AgNP@SiO_2 hybrid particles is attributed to the naked AgNPs and their teeth-like synergistic effect in a three-dimensional structure. Much like the case of AgNP@SiO_2/Fe_3O_4 hybrid particles,[20] the

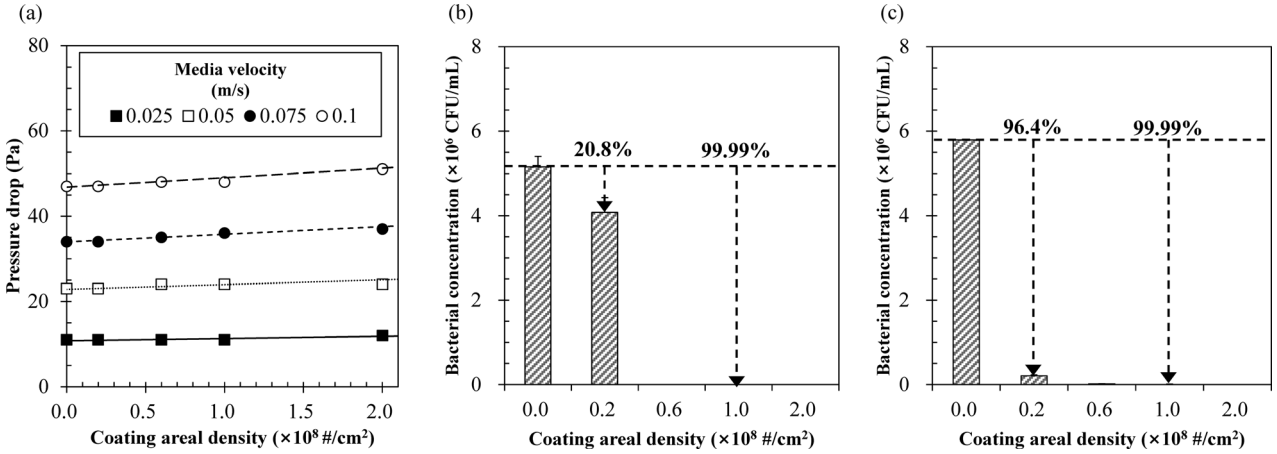

Fig. 3 (a) Pressure drop and antibacterial efficacy of AgNP@SiO_2-coated air filter samples for (b) *E. coli* and (c) *S. epidermidis*.

naked AgNPs chemically adsorb Mg^{2+} or Ca^{2+} ions from the Gram-negative bacterial membrane that contains tightly packed lipopolysaccharides (LPS). Within the membrane, metal ions such as Mg^{2+} and Ca^{2+} play an essential role in preserving the structure by strengthening the LPS interactions.[38] The same mechanism is also likely responsible for the efficacy against the Gram-positive bacteria. In the case of Gram-positive bacteria, the thick peptidoglycan layer of the cell wall is known to be resistant to the penetration of Ag^{+} ions.[8] However, the peptidoglycan layer is also strengthened by metal ions, as Mg^{2+} and Ca^{2+} ions are known to form bridges across phosphate groups in adjacent teichoic acid chains in the Gram-positive bacterial cell wall.[39] Thus, the naked AgNPs decorated on the silica sphere seem to pressurize the spots where the metal ions are bridged in the thick bacterial cell wall and chemically adsorb Mg^{2+} or Ca^{2+} ions, as observed on the right top side of Fig. 2b. Due to the thick bacterial cell wall, the bacteria stay attached to the AgNP@SiO_2 hybrid particles until they are disrupted by an external force, as indicated by the arrows in Fig. 2d and S6b.† From these images and the viability test in Fig. 3b and c, the trapped bacteria are assumed to be dead. Therefore, in both Gram-negative and Gram-positive bacteria, the bacterial trapping by AgNP@SiO_2 hybrid particles indicates cell death.

The air filter samples summarized in Table 1 all showed a coating efficiency of AgNP@SiO_2 particles greater than 90%. No meaningful detachments of AgNP@SiO_2 particles were observed from the coated air filter samples, even when a clean air flow of 10 L min^{-1} was forced onto them. In Fig. 3a, the pressure drops caused by the coating increased linearly with the increasing coating areal density at constant media velocity but are acceptable because the variation was generally within 5%. At a media velocity of 0.025 m s^{-1}, the filtration efficiencies of bioaerosols were 91% and 95% for the air filter samples with the coating areal densities of 6×10^7 and 2×10^8 # per cm^2, respectively. Although the CCM or the DDM do not exactly reflect antibacterial activity in air, we performed cell viability test using the CCM because there is no better alternative in the present case. In Fig. 3b and c, the antibacterial efficacies determined by the CCM were high (*i.e.*, >99.99%) against both *E. coli* and *S. epidermidis* in solutions containing the filter samples with a coating areal density $\geq 1 \times 10^8$ # per cm^2.

Conclusions

In conclusion, we have presented a large-scale (51 g) fabrication of highly monodisperse AgNP@SiO_2 hybrid particles and have shown their prompt and synergistic antibacterial activity against both Gram-negative and Gram-positive bacteria on air filtration units. The AgNP@SiO_2 hybrid particles showed antibacterial activity promptly and synergistically by the naked AgNPs on the silica sphere upon contacting bacteria. A further study on the antimicrobial effects using the AgNP@SiO_2-coated air filter and viruses showed promising results and will be published elsewhere. The hybrid particle AgNP@SiO_2 and the devices or appliances coated with the particles are expected to be useful for future green environment applications.

Acknowledgements

This research was supported by the Future-based Technology Development Program (Green Nano Technology Development Program) through the National Research Foundation of Korea funded by the Ministry of Science, ICT & Future Planning (Grant no. 2013-069323 and 2013-069325) and the KIST institutional program (Project no. 2E24860).

Notes and references

1 R. Maus, A. Goppelsröder and H. Umhauer, *Atmos. Environ.*, 2001, **35**, 105.
2 M. C. Verdenelli, C. Cecchini, C. Orpianesi, G. M. Dadea and A. Cresci, *J. Appl. Microbiol.*, 2003, **94**, 9.
3 C. Cecchini, M. C. Verdenelli, C. Orpianesi, G. M. Dadea and A. Cresci, *J. Appl. Microbiol.*, 2004, **97**, 371.
4 K. Y. Yoon, J. H. Byeon, C. W. Park and J. Hwang, *Environ. Sci. Technol.*, 2008, **42**, 1251.
5 E. Miaśkiewica-Peska and M. Łebkowska, *Fibres Text. East. Eur.*, 2011, **19**, 73.

6 S. J. Park and Y. S. Jang, *J. Colloid Interface Sci.*, 2003, **261**, 238.
7 J. H. Byeon, K. Y. Yoon, J. H. Park and J. Hwang, *Carbon*, 2007, **45**, 2313.
8 Q. L. Feng, J. Wu, G. Q. Chen, F. Z. Cui, T. N. Kim and J. O. Kim, *J. Biomed. Mater. Res.*, 2000, **52**, 662.
9 I. Sondi and B. Salopek-Sondi, *J. Colloid Interface Sci.*, 2004, **275**, 177.
10 M. Rai, A. Yadav and A. Gade, *Biotechnol. Adv.*, 2009, **27**, 76.
11 C. Marambio-Jones and E. M. V. Hoek, *J. Nanopart. Res.*, 2010, **12**, 1531.
12 S. Eckhardt, P. S. Brunetto, J. Gagnon, M. Priebe, B. Giese and K. M. Fromm, *Chem. Rev.*, 2013, **113**, 4708.
13 A. Kumar, P. K. Vemula, P. M. Ajayan and G. John, *Nat. Mater.*, 2008, **7**, 236.
14 C.-N. Lok, C.-M. Ho, R. Chen, Q.-Y. He, W.-Y. Yu, H. Sun, P. K.-H. Tam, J.-F. Chiu and C.-M. Che, *J. Biol. Inorg. Chem.*, 2007, **12**, 527.
15 O. Choi, K. K. Deng, N.-J. Kim, L. Ross Jr, R. Y. Surampalli and Z. Hu, *Water Res.*, 2008, **42**, 3066.
16 Z. Xiu, Q. Zhang, H. L. Puppala, V. L. Colvin and P. J. J. Alvarez, *Nano Lett.*, 2012, **12**, 4271.
17 W.-R. Li, X.-B. Xie, Q.-S. Shi, H.-Y. Zeng, Y.-S. OU-Yang and Y.-B. Chen, *Appl. Microbiol. Biotechnol.*, 2010, **85**, 1115.
18 G. A. Sotiriou and S. E. Pratsinis, *Environ. Sci. Technol.*, 2010, **44**, 5649.
19 A. Panáček, L. Kvítek, R. Prucek, M. Kolář, R. Večeřová, N. Pizúrová, V. K. Sharma, T. Nevěčná and R. Zbořil, *J. Phys. Chem. B*, 2006, **110**, 16248.
20 H. H. Park, S. Park, G. Ko and K. Woo, *J. Mater. Chem. B*, 2013, **1**, 2701.
21 L. Zhang, Q. Luo, F. Zhang, D.-M. Zhang, Y.-S. Wang, Y.-L. Sun, W.-F. Dong, J.-Q. Liu, Q.-S. Huo and H.-B. Sun, *J. Mater. Chem.*, 2012, **22**, 23741.
22 J. H. Byeon, B. J. Ko and J. Hwang, *J. Phys. Chem. C*, 2008, **112**, 3627.
23 K.-Y. Yoon, J. H. Byeon, J.-H. Park, J. H. Ji, G. N. Bae and J. Hwang, *Environ. Eng. Sci.*, 2008, **25**, 289.
24 B. U. Lee, S. H. Yun, J.-H. Ji and G.-N. Bae, *J. Microbiol. Biotechnol.*, 2008, **18**, 176.
25 Y. H. Joe, W. Ju, J. H. Park, Y. H. Yoon and J. Hwang, *Aerosol Air Qual. Res.*, 2013, **13**, 1009.
26 J. H. Jung, G. B. Hwang, J. E. Lee and G. N. Bae, *Langmuir*, 2011, **27**, 10256.
27 W. Stöber, A. Fink and E. Bohn, *J. Colloid Interface Sci.*, 1968, **26**, 62.
28 Y. Qian, K. Willeke, S. A. Grinshpun, J. Donnelly and C. C. Coffey, *Am. Ind. Hyg. Assoc. J.*, 1998, **59**, 128.
29 H. H. Park, K. Woo and J.-P. Ahn, *Sci. Rep.*, 2013, **3**, 1497, DOI: 10.1038/srep01497.
30 A. Kumar, H. Joshi, R. Pasricha, A. B. Mandale and M. Sastry, *J. Colloid Interface Sci.*, 2003, **264**, 396.
31 D. V. Leff, L. Brandt and J. R. Heath, *Langmuir*, 1996, **12**, 4723.
32 J. Liu, Z. Zhao, H. Feng and F. Cui, *J. Mater. Chem.*, 2012, **22**, 13891.
33 J. B. Jackson and N. J. Halas, *J. Phys. Chem. B*, 2001, **105**, 2743.
34 A. J. Bard and L. R. Faulkner, *Electrochemical Methods: Fundamentals and Applications*, John Wiley & Sons, Inc., New York, 2001, p. 808.
35 S. Joshi, G. S. Bisht, D. S. Rawat, A. Kumar, R. Kumar, S. Maiti and S. Pasha, *Biochim. Biophys. Acta*, 2010, **1798**, 1864.
36 W. Ziebuhr, C. Heilmann, F. Götz, P. Meyer, K. Wilms, E. Straube and J. Hacker, *Infect. Immun.*, 1997, **65**, 890.
37 D. Vujošević, M. Mozetič, U. Cvelbar, N. Krstulović and S. Milošević, *J. Appl. Phys.*, 2007, **101**, 103305.
38 N. A. Amro, L. P. Kotra, K. Wadu-Mesthrige, A. Bulychev, S. Mobashery and G.-y. Liu, *Langmuir*, 2000, **16**, 2789.
39 I. Sadovskaya, E. Vinogradov, J. Li and S. Jabbouri, *Carbohydr. Res.*, 2004, **339**, 1467.